PERGAMON

Atmospheric Environment 37 (2003) 1243–1259

ATMOSPHERIC ENVIRONMENT

www.elsevier.com/locate/atmosenv

Refinements to the particle-into-liquid sampler (PILS) for ground and airborne measurements of water soluble aerosol composition

Douglas A. Orsini[a], Yilin Ma[a], Amy Sullivan[a], Berko Sierau[b], Karsten Baumann[a], Rodney J. Weber[a,*]

[a] *School of Earth and Atmospheric Sciences, Georgia Institute of Technology, Atlanta, GA, USA*
[b] *Institute for Tropospheric Research, Permoserstr. 15, Leipzig, Germany*

Received 17 July 2002; accepted 5 November 2002

Abstract

An improved particle-into-liquid sampler (PILS) has proven successful in both ground-based and aircraft experiments for rapid measurements of soluble aerosol chemical composition. Major modifications made to the prototype PILS (Aerosol Sci. Technol. 35 (2001) 718) improve particle collection at higher sample flow (15–17 l min^{-1}) while maintaining minimal sample dilution. Laboratory experiments using a fluorescent calibration aerosol aided in designing the present system and characterized the PILS collection efficiency as a function of particle size. Collection efficiency for particle diameters D_p between 0.03 and 10 μm is greater than 97%. In addition, the instrument now samples at low pressures (0.3 atmosphere) necessary for airborne measurements up to approximately 8 km in altitude. An ion chromatograph (IC) is coupled to the PILS for direct on-line analysis of the collected sample (hence the name 'PILS-IC'). Proper selection of columns and eluants allows for 3.5–4 min separation of 9 major inorganic species (Na^+, NH_4^+, K^+, Ca^{2+}, Mg^{2+}, Cl^-, NO_3^-, NO_2^-, SO_4^{2-}), while acetate, formate, and oxalate, are also possible in 15 min. Any analytical technique capable of continuous online analysis of a liquid sample can be coupled to the PILS for quantitative semi-continuous measurements of aerosol composition. Changes made to the prototype are explained and data from a recent experiment are compared with standard integrated filter measurements.

Keywords: Particulate matter; PM2.5; Instrumentation; Ionic aerosol components; On-line analysis

1. Introduction

Atmospheric measurements of particle chemical composition provide insight into aerosol sources and atmospheric transformation processes. Although traditional filter methods are widely used both in ground-based and airborne studies, a variety of semi-continuous instruments have been developed which measure on a much faster time-scale (Boring et al., 2002; Khlystov et al., 1995; Simon and Dasgupta, 1995; Slanina et al., 2001; Stolzenburg and Hering, 2000; Turpin et al., 1990; Weber et al., 2001). The Atlanta Supersite experiment in August 1999, provided a unique platform to inter-compare the newer techniques (Lim et al., 2002; Weber et al., 2003b). The highly time-resolved methods show changes in aerosol chemistry not observable in data sets provided by filters. For example, in the Atlanta Supersite experiment, the semi-continuous instruments chemically speciated ubiquitous short-lived fine particulate matter (PM) events, otherwise lost in the long averaging times of the filters (e.g. 24 h) (Weber et al., 2003a).

Several instruments recently developed, often referred to as 'steam collection devices', use the technique of

*Corresponding author.

1352-2310/03/$ - see front matter
doi:10.1016/S1352-2310(02)01015-4

growing aerosol particles into droplets in a supersaturated environment of water vapor. In this way, the grown droplets are large enough for collection by inertial techniques and subsequent online or offline analysis. Many of these systems also allow for the simultaneous detection of gas phase species using wet denuders. Simon and Dasgupta (1995) developed one of the first instruments by mixing steam with aerosol particles in a 10 l min^{-1} sample flow. The particles were further grown in a cooled stainless steel maze and collected from the air in a gas/liquid separator. Coupled to a concentrator column and ion chromatography (IC), a sulfate LOD of $\sim$2 ng m^{-3} was attained for an 8 min sampling time. Further variations on this design have also evolved (Zellweger et al., 1999, 1997; Löflund et al., 2001). At the same time, a system was also developed in the Netherlands called the Steam Jet Aerosol Collector (SJAC) (Khlystov et al., 1995; Slanina et al., 2001). This system, which has seen wider use in Europe, collects grown droplets and condensed water vapor in a cyclone for online IC-analysis using a preconcentrator column. For a sample flow rate of 20–60 l min^{-1}, the LOD of the SJAC ranges from 20 to 50 ng m^{-3}. Another system, developed by Kidwell and Ondov (2001), grows particles in a high aerosol sample flow (170 l min^{-1}) followed by droplet concentration using a combination virtual/real impactor. The collection technique allows for increased lower detection limits (LOD) ($\sim$1 ng m^{-3}), for online analysis of trace metals in aerosols using Graphite Furnace Atomic Absorption Spectroscopy. Further analysis techniques have also been applied to collection of grown droplets in a system called the condensational-growth and impaction system (C-GIS). (Sierau et al., 2002). In this instrument, 1.5–2 l min^{-1} of an aerosol sample flow is saturated with water vapor that further condenses on the particles in a laminar flow tube. The different techniques of offline analysis applied to the impacted droplets included capillary electrophoresis combined with UV-detection (CE-UV) and CE combined with electrospray (ion trap) mass spectrometry (CE-ESI-MS). Speciation of organic PM is possible in sampling times less than 10 min. As part of the 1999 Atlanta Supersite Experiment, a prototype particle-into-liquid sampler (PILS) coupled to a dual channel IC measured concentrations of the major soluble inorganic ions in the $PM_{2.5}$ aerosol. Online collection of the impacted droplets was possible by adding an adjustable transport flow to the impactor (0.05–0.1 ml min^{-1}), which continually washed the droplets from the surface and filled sample loops for online IC analysis. With a measurement every 7 min, the LOD for the detected ion species was 0.1 μg m^{-3}. The positive results from this study encouraged further development of the PILS, conceived as an instrument to rapidly speciate and quantify soluble aerosol composition.

Fig. 1 shows the collection efficiency curve for the prototype PILS obtained from laboratory-generated aerosols. The calibration aerosol, generated by an atomizer and differential mobility analyzer (DMA) (Knutson and Whitby, 1975) was measured by the PILS and simultaneously scanned with a scanning mobility particle spectrometer (SMPS Model 3934, TSI Inc., St Paul MN). The efficiency curve drops-off for $D_p < 0.1$ μm due to poor activation efficiencies of the smaller particles. No attempt was made in these earlier experiments to determine the upper size limit of this instrument. Intercomparisons of $PM_{2.5}$ nitrate and sulfate based on the Atlanta Supersite experiment did show, however, that the prototype PILS agreed well with other semi-continuous instruments (relative difference 30% for nitrate, 11% for sulfate) and with 24-h integrated filter measurements (18% for nitrate, 19% for sulfate) (Weber et al, 2003b).

2. PILS operating principle

The idea behind the PILS is to collect ambient particulates into a small stream of high purity water, thereby producing a solution containing the aerosol species sampled at a certain moment in time. This is accomplished by first mixing an ambient aerosol sample flow (15–17 l min^{-1}) with a smaller turbulent flow of 100°C steam ($\sim$1.5 l min^{-1}). Rapid adiabatic cooling of the warmer turbulent steam by the cooler ambient sample gives a high supersaturation of water vapor. In this supersaturated environment, the aerosol particles grow into droplets ($D_p > 1$ μm) large enough to be collected by an impactor. The droplets are collected to produce a continuous liquid flow for online analysis of the species in solution. Any technique capable of continuous online analysis of the liquid sample can record the changing aerosol composition. Since ambient gases also present in the aerosol sample might contribute to the particle phase measurement, it is necessary to place denuders inline, upstream of the PILS to remove gas phase species. (This is described in more detail later.)

The modifications made to the prototype PILS to improve its collection efficiency, have led to several intermediate versions of the device. These efforts, combined with an array of laboratory tests, produced the latest version of the PILS, which is considerably different from the original prototype. Described here, are two versions of the device. First, an intermediate PILS, which recounts the initial design changes, and second, the most recent version, whose construction was aimed at solving the issues in the intermediate stage.

2.1. The designs

Since our last report (Weber et al., 2001), an intermediate PILS was designed to improve steam

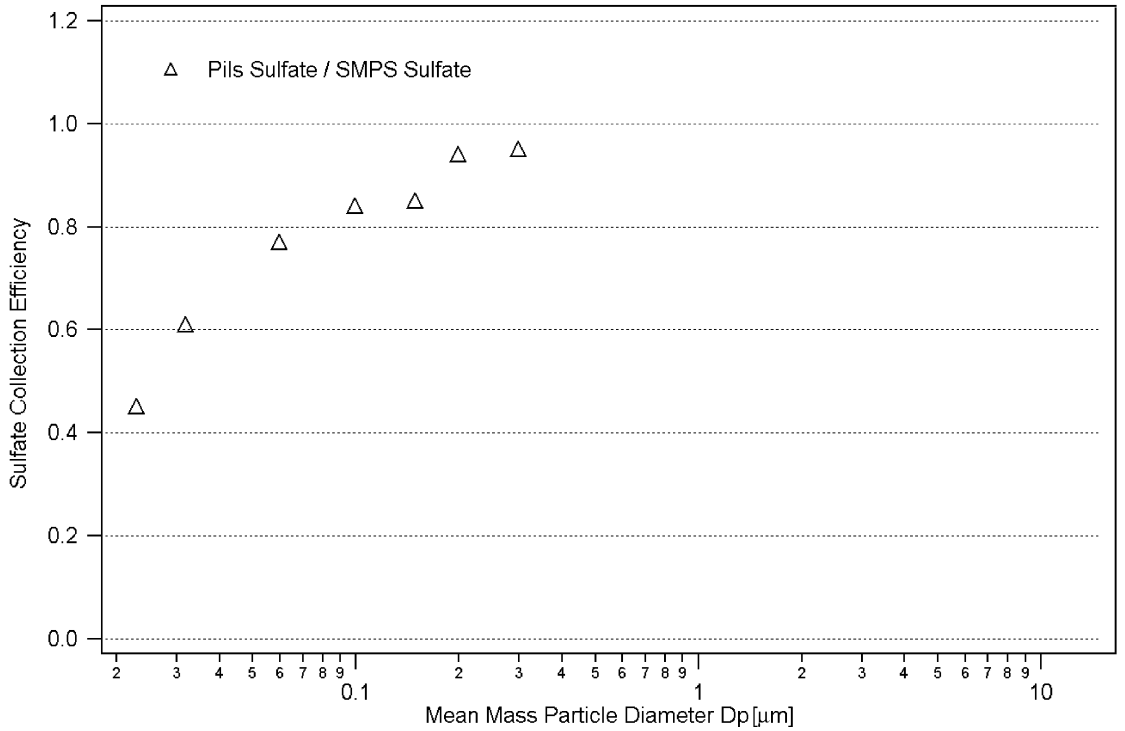

Fig. 1. Calibration curve from the original prototype PILS. Calibration was made by generating a monodisperse ammonium sulfate aerosol and scanning the mass with a scanning mobility particle sizer (SMPS).

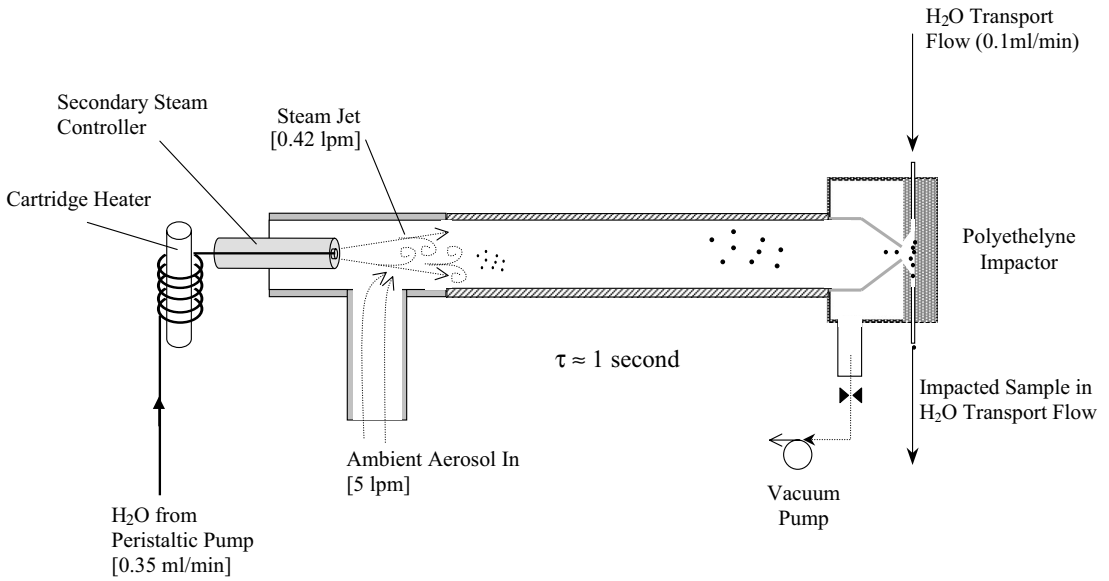

Fig. 2. Intermediate 5 l min^{-1} PILS design.

generation and droplet collection (Fig. 2). A new secondary steam controller was built to maintain a constant steam temperature and steady flow. Like the prototype, the steam flow rate is still controlled by the flow rate of DI water through a cartridge heater. In this version however, an orifice inserted into the end of the steam nozzle creates a backpressure to suppress the unstable boiling of the water. At the tip of the nozzle

where the steam exits, a thermocouple and PID controller were added to maintain the temperature of the steam to within $\pm 0.5^{\circ}$C. We found this control necessary to properly define the conditions of super saturation needed for particle activation and subsequent steady growth. The second modification to the PILS was in impactor design. Originally, the aerosol sample was impacted on a glass surface and contained within an area that was wetted by the droplets. This design was unreliable however since effective transport of the liquid sample was dependent on the wetting of the glass surface. Furthermore, since the volume of the collected liquid is small, reducing the area onto which it is collected is one of the key factors in concentrating the sample for analysis. In the intermediate impactor design, the area onto which the aerosol sample impacts was physically contained within a small cavity cut out of a polycarbonate endcap. This construction physically contained the droplets to within the cavity area and allowed for a reduced flow of deionized water across the surface ($<0.1\,\mathrm{ml\,min^{-1}}$).

The most recent design of the PILS (Fig. 3) was motivated by the desire for aircraft deployment as well as to sample behind the EPA standard sample flow of $16.7\,\mathrm{l\,min^{-1}}$. For the case of an increased sample flow, more steam is required to activate the aerosol while maintaining rapid and complete mixing. Reynolds numbers are therefore higher and the risk of droplet loss due to turbulent deposition increases.

In the most recent PILS, the steam generator differs in that the vapor is forced through a 5 cm (2 in) long 1.58 mm (1/16 in) o.d. tube with a 0.381 mm (0.015 in) i.d. This allows for a 90° bend in the 5 cm tube to direct the steam along the centerline, parallel to the sample flow that enters along a straight path from the back of the PILS. The small diameter of this tube inhibits heating of the sample air and cooling of the steam prior to mixing, both of which reduce the final degree of vapor saturation once mixed. The end of the steam tube is also housed in a Teflon sheath to further help reduce heat transfer to the sample and to hold a thermocouple which monitors the steam temperature at the point of injection into the ambient air flow. Inside the PILS, the turbulent jet of steam mixes with the ambient sample at the apex of a conical expansion. The wall expansion reduces the flow velocity and allows for spreading of the steam jet to reduce vapor loss by immediate condensation to the wall.

The 15 cm (6 in) long by 5 cm (2 in) wide body of the PILS is passively air cooled with fins and provides an approximate 1-s residence time. As will be shown, this is sufficient for the particles to grow larger than 1 μm. The

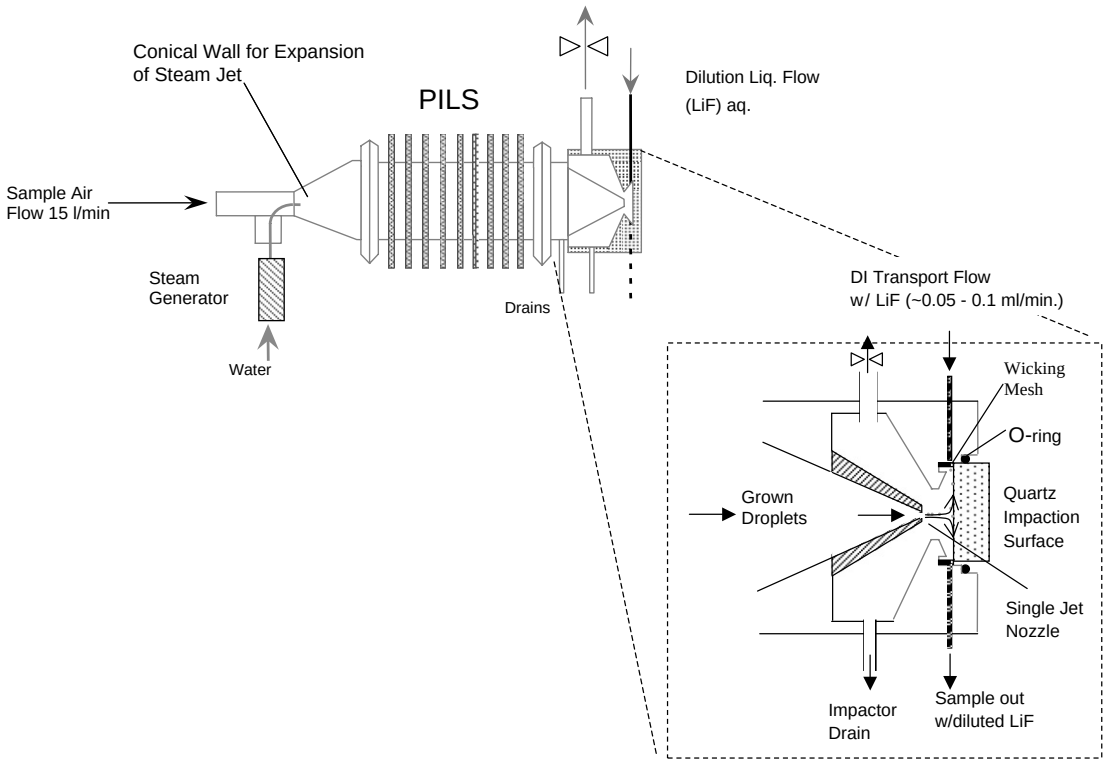

Fig. 3. Schematic of the new $15\,\mathrm{l\,min^{-1}}$ PILS design.

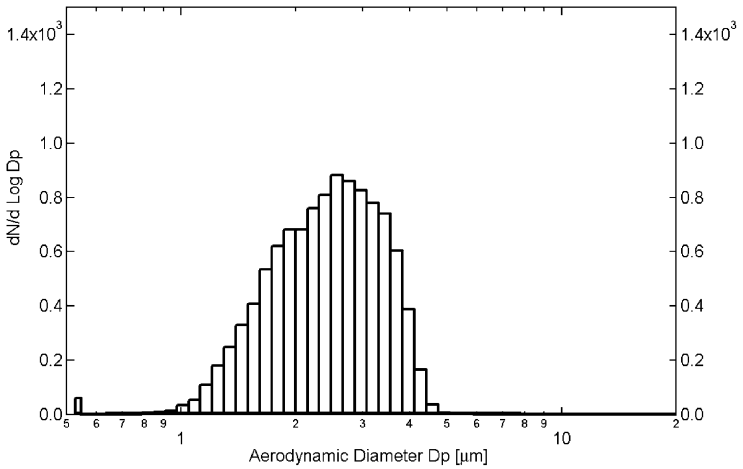

Fig. 4. Number droplet distribution measured by an aerodynamic particle sizer (APS) attached to the end of the PILS body. Aerosol sample is ambient room air.

final particle size depends on the initial conditions (temperature and relative humidity) of the two merging flows and their mass flow rates. Fig. 4 shows a typical size distribution of droplets emerging from the PILS while sampling room air in the Georgia Tech lab. The recorded data in Fig. 4 is a 10-s average measured with an Aerodynamic Particle Sizer (APS, TSI St. Paul MN) attached to the end of the growth chamber. After the aerosol particles are grown in the PILS, they are focused by a tapered wall into a single nozzle, the tip of which extends slightly into a conical-shaped cavity. The nozzle directs the sample flow containing the droplets against a quartz surface inside the cavity to achieve a 1-μm diameter cut size. (Marple and Willeke, 1976; Rader and Marple, 1985). The radially spreading jet of air forces the impacted droplets to the perimeter of the quartz plate. The quartz serves well because it is highly wettable, allows for viewing the impacted drops, and minimizes background sodium ion (Na^+) concentrations, which we observed with regular silica glass. A narrow ribbon of stainless-steel mesh or similar wicking material is placed in a groove at the outside edge of the impaction surface to wick the liquid away from the plate as soon as it reaches the perimeter. A small selectable flow of high purity deionized water introduced at the top of the cavity, travels along the wick and transports the collected liquid to an exit tube at the base of the impactor. The final exiting flow is a solution containing the soluble ions of the collected aerosol particles. In field studies where the PILS has been interfaced to an IC, the flow of the transport liquid entering the impactor has ranged from 0.03 to 0.1 ml min^{-1} to accommodate filling 150–500 μl sample loops. A slower flow results in a more concentrated exit solution for analysis, however this somewhat depends on the duty cycle and liquid flow requirements of the analytical technique used.

During collection, liquid from the transport flow and droplets dilute the sample. In addition, a small amount of water condenses-out of the saturated air, which passes over the cooler quartz impaction surface. This additional water typically ranges between 5 and 20 μl min^{-1}. To account for the dilution due to condensation, the incoming transport flow is spiked with a known concentration of lithium fluoride or related non-interfering ions. By measuring the diluted lithium and/or fluoride exiting the impactor, the added water is taken into account and the measured aerosol concentration is completely quantifiable, calculated with the following equation:

$$[C_g] = [C_L] q_{in} R / Q_a, \quad (1)$$

where: $[C_g]$ is the ambient aerosol concentration (μg m^{-3}), $[C_L]$ is the concentration of the ion in the collected sample liquid (μg l^{-1}) (For ion chromatographic analysis, this is determined from calibrations with NIST-traceable ion standards in aqueous solutions), q_{in} is the flow of the spiked transport liquid entering the top of the impactor (μg l^{-1}) (typically 0.05 to 0.1 ml min^{-1}), R the ratio of the spiked species concentration (e.g. Li^+) entering the impactor divided by the concentration exiting the impactor (this ratio accounts for the sample dilution), and Q_a the volumetric flow rate of sample air entering the PILS (l min^{-1}).

3. Calibrations

During various stages of developing the new design, a series of tests were undertaken to determine the performance of the modified PILS. This included side-by-side comparisons with the original prototype whose performance had been verified as part of the Atlanta

Supersite experiment (Weber et al., 2003b). Here we focus on calibration of the intermediate and recent designs that characterize the steps taken to improve the instruments' performance. In a final section, comparisons between ambient measurements made with the intermediate PILS and 24-h integrated filters are presented.

In order to calibrate the size-dependent collection efficiency of the PILS, two standard methods of particle generation were needed to cover the large particle size range (Fig. 5). For diameters $D_p > 1\,\mu m$, a vibrating orifice aerosol generator (VOAG 3450, TSI Inc, St Paul MN) produced particles out of a solution of olive oil (0.1–10%) and propanol, tagged with a small amount of fluorescein (0.01%, Aldrich Chemical). The size of the particles generated depended on the fraction of olive oil in solution and the VOAG operating frequency. Shown in Fig. 5, the VOAG was turned upside-down to maximize transport of large particles in $\sim 2\,l\,min^{-1}$ of nitrogen dilution air. A neutralizer placed in the dispersion tube reduced particle loss due to electrostatic effects. An APS, located just before the PILS, monitored the diameter of the generated aerosol. To accommodate the total flow of the PILS and APS, $18\,l\,min^{-1}$ of dried ambient room air was added. The purpose of the dried make-up air was to more closely mimic field operation by embedding the calibration aerosol in a dry ambient aerosol while testing the collection efficiency at low relative humidity. No sensitivity to relative humidity was found for RHs ranging from 10% to 40%.

For particles $D_p < 1\,\mu m$, an atomizer in series with a DMA generated a polydisperse aerosol also from a solution containing fluorescein. An impactor inline following the DMA removed doublets and larger particles before being scanned with an SMPS. In calibration of the most recent PILS, an after-filter placed downstream collected any particle mass that penetrated the entire instrument. The relative particle loss inside the PILS was determined by washing out the fluorescent mass from the separate components followed by analysis with a fluorimeter (Shimadzu RF-Mini 150). The collection/deposition of fluorescent mass in the PILS, which was visible to the naked eye, was diluted by a factor of 1000 by pipetting 20 μl of each collected sample into 20 ml of ultrapure water. This made it possible to analyze each extraction within the picogram range of the fluorimeter, and also reduced the likelihood of artifacts from mass that may have not been extracted entirely or leftover from the previous run. The four

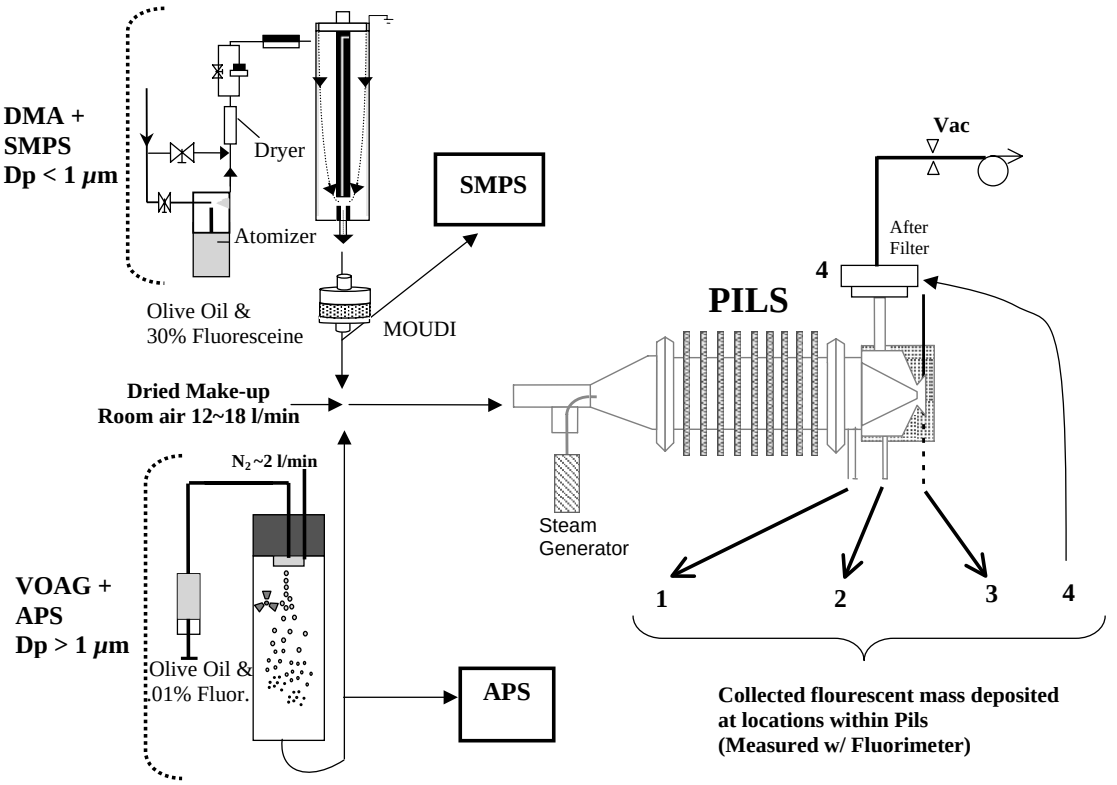

Fig. 5. Schematic of the laboratory set-up to generate a fluorescent calibration aerosol. Vibrating orifice aerosol generator (VOAG) aerosol diameter (D_p) was monitored with an APS. DMA aerosol distribution was scanned with an SMPS.

separate regions of collected fluorescein and the possible reasons for deposition are (see Fig. 5):

1. *Body of PILS*: Deposition due to turbulent loss and gravitational settling of droplets;
2. *Impactor loss*: Droplet deposition inside the inner nozzle plus impacted droplets not collected in the impaction cavity;
3. *Collected sample*: Mass collected by the impactor in continuous flow for analysis;
4. *Penetrated mass*: All mass not removed by PILS and collected on filter. (Applied to 15 l min^{-1} PILS only).

Fig. 6 shows the efficiency curves for the prototype, intermediate, and recent PILS designs. Each point represents an average of three measurements. For the 5 l min^{-1} intermediate PILS, the efficiency test was only performed for the upper size range from D_p 0.2 to 6.0 μm. In this version, the estimated 50% collection efficiency was 2.8 μm, at which point droplet loss increased steeply within the body. For the 15 l min^{-1} PILS, the collection efficiency is greater than 95% from 0.03 to 6.0 μm and begins to drop-off at $D_p \sim 10$ μm. A D_{p50} is estimated at ~ 11 μm. It should be noted, that with a single jet nozzle, a jet velocity of approximately 6200 cm s^{-1} is needed for a cut size of 1 μm. Calculation of the Weber Number ($Wb = 133$) does show that the drops should break-up upon impaction. It seems unlikely however, that the small liquid drops produced by shatter would bounce back or afterwards follow the air streamlines and not be collected. Based on the calibrations, apparently this does not result in a loss of liquid downstream of the impactor. Instead the loss of collected mass is observed within the body of the PILS. For particles $D_p < 1$ μm there is not any appreciable loss down to ~ 30 nm. The gap in the graph near $D_p \sim 1$ μm, results from the size limits of the two aerosol generation techniques.

4. Discussion of modifications

4.1. Lower size limit

In the prototype PILS, the decreased collection efficiency for particles $D_p < 0.1$ μm, shown in Fig. 1, was believed to be the result of poor mixing of steam and ambient air. Poor mixing can result in low vapor supersaturation and limited particle activation. An unsteady flow of water vapor with minimal turbulence was the most probable cause. The first changes to improve mixing were incorporated into the intermediate design. The steam generator was developed to produce a steady, high velocity flow of water vapor (Reynolds number ~ 4000) to achieve rapid near-adiabatic mixing with the

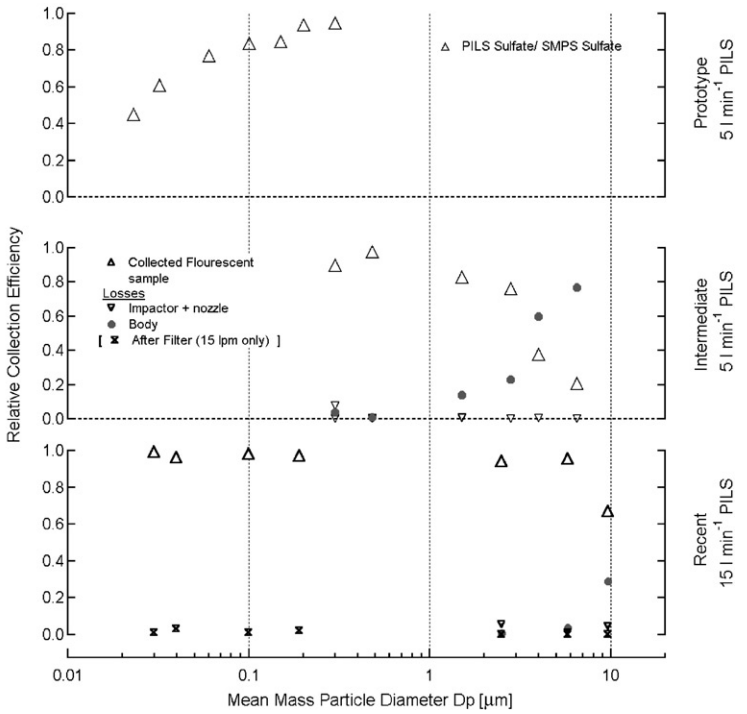

Fig. 6. Calibration curves of particle collection efficiency as function of particle diameter, D_p.

aerosol sample and to maximize the super-saturation. In the recent version, although the design of the generator was modified, this turbulent steam jet was incorporated into the recent version to maintain the same degree of mixing.

4.2. Upper size limit

Experiments with fluorescent calibration aerosols made possible the direct visual observation of particle collection and loss within the PILS. This enabled the testing of design changes on-the-spot and aided greatly in our understanding of the droplet loss in the PILS. In the intermediate design, we observed the fluorescent aerosol to suffer heavy losses due to turbulent deposition when it entered perpendicular to the direction of the steam flow (see Fig. 2). This problem was compounded by the expansion of the turbulent steam jet against the inner walls of a 1.27-cm (0.5 in) i.d. tube, resulting in poor collection efficiency of particles $D_p > 1.3\,\mu m$. In the present design, the conical expansion in the wall of the PILS at the point of steam injection and mixing reduces droplet transport to the wall. In addition, the aerosol sample enters parallel to the flow of steam, eliminating the 90° turn. With these geometry changes, and while maintaining a high Reynolds number steam jet, the upper size cut of the PILS was increased from 2.8 to 11 μm with an increased sample flow from 5 to $15\,l\,min^{-1}$. Large particle losses are again observed as droplet deposition within the body.

5. Impaction and collection

Two types of impactors have been used for droplet collection in the $15\,l\,min^{-1}$ PILS. Initially, a 5-jet nozzle was employed to lower the jet velocity and pressure drop across the impactor. With multiple jets however, approximately 13% of the aerosol mass ($D_p < 1.3\,\mu m$) was deposited in the upstream side of the nozzle at the point where flow splitting occurred. Our goal to increase the collection efficiency and to include larger diameter particles led to the development of a single jet impactor (see Fig. 3a). The adoption of a single jet is tricky, however, because the higher jet velocity spatters the impacted sample, rendering 100% liquid collection impossible. The success of this design relies on removal of the collected liquid from the impaction plate as soon as possible to avoid build-up. Several wettable materials were tested to facilitate removing the liquid in a continuous manner for analysis. In the present design a strip of quartz glass or stainless steel mesh (477 μm pore size) placed at the outside of the impaction cavity wets easily and wicks the liquid away as soon as it spread to the perimeter. The wicking of this liquid is so strong that the orientation of the impactor is not important, thus making extraction of the sample liquid possible from the top of the impaction plate.

6. Ion chromatography

To a large extent, the analytical technique determines both the sampling rate (i.e., duty cycle) at which species can be detected, and the lower detection limits. Up until this time, IC has been the primary means of online analysis of the sample flow because it allows for quantitative speciated inorganic and organic analysis depending on the type of separation column used. A Metrohm IC (Compact 761, Metrohm, Herisau,, Switzerland) was chosen for its simplicity, compactness, and adaptability in the field. The instrument has also proven reliable in continuous monitoring.

The underlying limitation in the sampling rate of the PILS-IC system is determined by the duty cycle of the IC, or the ability of the column to adequately separate the species of interest. The trade off with IC analysis is between the number of analytes eluted and sampling time. IC is often not a fast analysis technique, however selection of appropriate columns and eluants has enabled sampling rates of the major ions as fast as 3.5 min. Table 1 summarizes combinations of columns and eluants that we have successfully used in ground-based and aircraft studies.

For the sake of simplicity and robust field operation, we use sample loops to collect the liquid for IC injection versus concentrator columns, as done in other techniques (Boring et al., 2002; Slanina et al., 2001). In this case, the volume of the injected sample represents the average chemical composition during the time of filling. Between injections, the fill-time is constrained by the duty cycle of the IC, which in turn constrains the selection of sample loop volume and flow rate of liquid generated by the PILS (related to q_{in}). In recent aircraft studies, for example, separation of major inorganic ions is possible within 4 min using a 150 μl sample loop and a transport liquid flow $q_{in} < 0.08\,ml\,min^{-1}$, which is split between two ICs. In ground-based studies, where speciated organic acids are desired, 150–500 μl sample loops have been used and filled within 15–30 min duty cycles using various q_{in}.

6.1. Field operation

A schematic of the field operation of the PILS is shown in Fig. 7. Ideally, the PILS should sample as close to ambient conditions as possible to minimize volatility losses during sample transport to the instrument. In order to remove both organic and inorganic interference due to gases (e.g. SO_2 interpreted as SO_4^{2-}),

Table 1
Combinations of columns and eluants to measure specific ions in the PILS liquid

	Column	Eluant	Ions	Chemically suppressed	Time eluted [min]	Sample loop volume [μl]
Anions	Metrosep Supp 5–100 × 4.0 mm	4 mM Carbonate/ 1 mM bicarbonate	Cl^-, NO_3^-, SO_4^{-2}, HPO_4^{-2}, NO_2^-	Yes	3.5–4	150
	Supp 5–250 (+star anion)	5 mM Carbonate/ 1 mM bicarbonate	Cl^-, NO_3^-, SO_4^{-2} HPO_4^{-2}, NO_2^-, Acetate, Formate, Oxalate, (MSA)	Yes	15 (30)	500
Cations	Metrosep cation 1–2	4 m ML-Tartaric (or 2 mM nitric acid) 1 Mm dipicilinic acid	Li^+, Na^+ NH_4^+, K^+, Ca^{+2}, Mg^{+2}	No	3.5–4	150
	Metrosep Cation 2100 B- 100 × 4.0 mm–7 μm	0.25 g^{-1} Dipicolinic/ 1000 μl 1 2 N nitric/ 275 ml l^{-1} acetronitrile	Li^+, Na^+ NH_4^+, K^+, Ca^{+2}, Mg^{+2}	No	15	500
	Metrosep cation 2100	2.5 mM MSA	Li^+, Na^+ NH_4^+, K^+, Ca^{+2}, Mg^{+2}	No	15	500

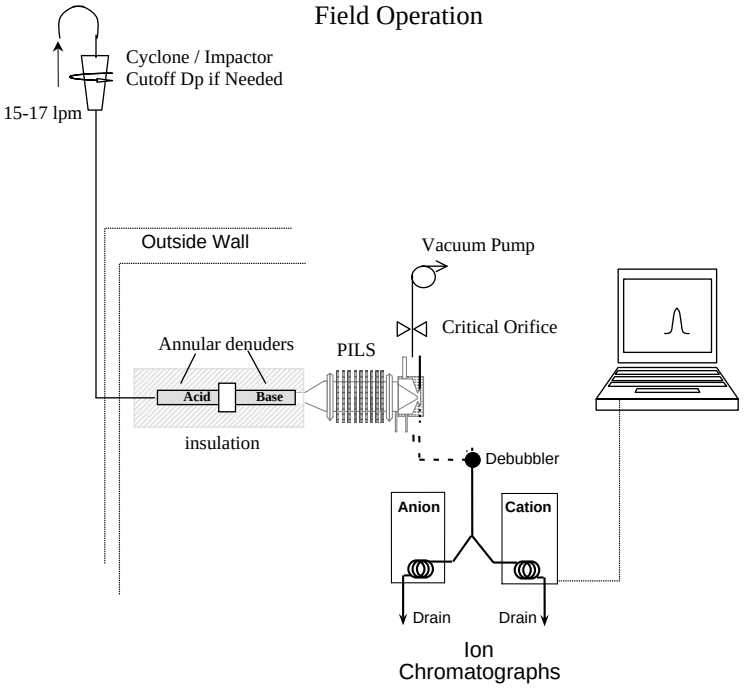

Fig. 7. Schematic of PILS set-up for field operation.

denuders must be placed inline immediately upstream of the PILS. Two annular glass denuders (URG-2000-30 × 242-3CSS) are coated with one of two solutions for the removal of gases. For the removal of the acids (HNO_3, HNO_2, SO_2, acetate, HCl, formic and oxalic acid), a coating solution is used containing 2% sodium carbonate in a solution of 500 ml deionized water, 20 ml of glycerol, and 750 ml of methanol. For the removal of NH_3, phosphoric acid is substituted for the sodium carbonate. At a flow rate of 15 l min^{-1}, the denuders are changed-out after 1 week of continuous operation. If necessary, a filter placed upstream of the denuders to eliminate the particles will verify if any unwanted gas is penetrating the denuder and interfering with the

baseline. This will also produce a 'blank' in ambient running conditions, which is periodically measured during field operation.

Our experience in past field studies has shown that with 18.3 MΩ deionized water used as the transport flow to fill two 150 μl sample loops, sulfate and nitrite are the two species which are sometimes detectable above the baseline noise during blank runs. The sulfate peak originates from our DI water, and varies from non-detectable to concentrations less than $5\,\mu g\,l^{-1}$. In the worst case, this translates to a background of $0.05\,\mu g\,m^{-3}$ of sulfate at standard measurement conditions. Background nitrite is not always present and possibly originates from an artifact associated with steam collection systems that has previously been reported (Boring et al., 2002). Standard denuders prepared with acidic and basic coatings likely do not remove gas phase NO_x (NO and NO_2), which potentially contributes to particulate nitrite through the following reaction in the warm droplets formed in the PILS:

$$NO_2 + NO + H_2O \rightarrow 2HONO \quad (3)$$

HONO is detected as nitrite (NO_2^-) with the IC. Although little evidence for this was observed in the Atlanta Supersite experiment (Weber et al., 2003b) we have occasionally observed higher background NO_2^- levels than other species. However, by employing a multi-channel denuder constructed of activated carbon (MAST Carbon Ltd., Surrey UK), this background NO_2^- was removed, suggesting the use of such denuders may essentially eliminate this interference. Furthermore, the use of the carbon denuder upstream of our standard coated glass denuders greatly extends the time between recoatings.

6.2. Limits of detection and sensitivity

To determine the limits of detection (LOD), the level of noise in the baseline must be known. This noise depends on the running conditions of the IC, which includes the type of column and eluant used, whether the eluant is degassed, the quality of deionized water, and IC internal temperature. For each instrumental set-up therefore, the detection limits should be determined. In Table 1, for example, while the substitution of nitric acid for tartaric acid in the Metrosep 1–2 column improves the separation of the cations Na^+ and NH_4^+, one ends-up with a noticeably noisier baseline, sacrificing the LOD. Fig. 8 displays both cation and anion baselines under field 'blank' conditions with the columns listed. For this configuration, the cation baseline noise is noticeably larger, and tends to drift at longer retention times. The Metrohm anion IC uses chemical suppression to increase the signal to noise ratio of the ionic species relative to the eluant. This is accomplished by the exchange of protons from a membrane regenerated with sulfuric acid (0.4 N solution). For the positive species however, the direct conductivity of the species relative to the eluant is already higher than with chemical suppression, hence the system is non-suppressed. For the example traces shown, the LOD were estimated by taking the mean of the peak areas integrate-able in the noise plus 3 times the standard deviation. Since each ion has a different conductivity response, some species will have better LOD than others. Without consideration of suppression or variability in the baseline noise, the pattern should in general follow the ion conductivity values listed in Table 2. This is more or less the case for the anions, where the baseline noise remains relatively steady. For the cation however, the baseline tends to drift slightly beyond 6 min elution time, lowering

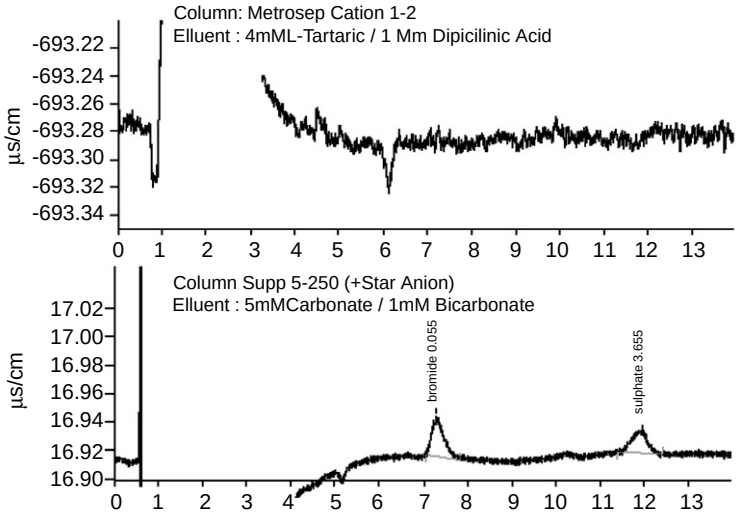

Fig. 8. Anion and cation 'blank' chromatograms during typical field operation.

Table 2
Determination of lower detection limits of ambient species is the 2nd from right column liquid concentration

	Species	Area + 3 × Std. Dev. (μS/cm s)	Ionic Conductivity[a] at 25°C ($S\,cm^2\,mol^{-1}$)	Concentration ($\mu g\,l^{-1}$)	Translated ambient conc. ($\mu g\,m^{-3}$)
Anions *(chemically suppressed)*	Cl^-	0.009	76	0.04	0.001
	NO_2^-	0.009	72	0.12	0.003
	Br^-	0.009	78	0.17	0.005
	NO_3^-	0.009	71	0.13	0.004
	$H_2PO_4^-$	0.009	33	0.28	0.008
	SO_4^{2-}	0.009	160	0.09	0.002
Cations *(non-suppressed)*	Li^+	0.065	39	0.15	0.004
	Na^+	0.091	50	0.64	0.017
	NH_4^+	0.256	73	2.20	0.059
	K^+	0.563	74	10.79	0.288
	Ca^{2+}	0.563	120	5.55	0.148
	Mg^{2+}	0.563	106	2.44	0.065

[a] From Metrohm monograph 50413.

the LOD of those species with longer retention times. The $\mu g\,l^{-1}$ concentrations stated in the table are based on the concentration values of the smallest injected standard of each species. The results are summarized. Accuracy is the measure of how close a measurement comes to the true value. In a later discussion, an inter-comparison with filters is taken as a measurement of PILS accuracy relative to the filters; in this case what is taken to be the reference. Precision on the other hand, is an indicator of an instrument's ability to replicate a measurement (Willeke and Baron, 1997). In a recent field study, two $15\,l\,min^{-1}$ PILS ran side-by-side, which allowed us to observe the instrument-to-instrument variation, and to some extent, quantify the precision. Differences between the instruments must first be minimized according to the standard operating procedure (SOP). This includes for example, accurate sample flow measurement and IC calibration. Fig. 9 shows the ambient inter-comparison data in the concentration range of 4–10 $\mu g\,m^{-3}$. The correlation coefficient r^2 describes how well the two measurements vary with one another. In this case, $r^2 = 0.96$, and therefore 96% of the variance in PILS 1 is observed in PILS 2. The outside lines represent the 99% confidence range within which the measurements agree based on the data shown. Between 4 and 10 $\mu g\,m^{-3}$ therefore, we expect with 99% confidence, the precision of the PILS to be within 0.4 $\mu g\,m^{-3}$.

7. Example results from recent field studies

7.1. Comparisons with integrated filters

The standard technique for measuring aerosol chemical composition has traditionally been the extraction of collected mass from filters. In a recent field study (TEXAQS 2000, Houston, TX), the intermediate $5\,l\,min^{-1}$ version of the PILS was directly compared against 24-h integrated filter measurements of $PM_{2.5}$ sulfate, ammonium, and nitrate are shown in Figs. 10–12. The time series plots show the extreme concentrations seen in the fast data that are washed-out in the filter averages. The regression analysis of the PILS data merged to the filter is compared only for those periods where the PILS covered $\geqslant 85\%$ of the filter averaging time. For sulfate, the linear regression slope and intercept of the PILS versus the Filter were 1.03 ± 0.02 and $0.14 \pm 0.01\,\mu g\,m^{-3}$, with an r-value of 0.98. The uncertainty corresponding to the slope and intercept is that associated with a 95% confidence interval. For ammonium, the slope and intercept were 0.93 ± 0.01 and $0.24 \pm 0.02\,\mu g\,m^{-3}$, with an r-value of 0.94. For nitrate, the agreement between the PILS and filter is poor. It can be seen in the lower time series graph for the nitrate, that for high values of the filter ($> 0.5\,\mu g\,m^{-3}$), the PILS nitrate is low, and for low values of the filter, the PILS data is highly scattered. It is likely that the poor nitrate comparison for low values is due to the ambient nitrate concentrations being typically less than $1\,\mu g\,m^{-3}$, approaching the filter detection limit. In the Atlanta Supersite study, Weber et al. (2003b) compared the on-line semi-continuous instruments, including the prototype PILS, and found better agreement amongst themselves than similar comparisons against the integrated filters. In that study, the PILS regression to the mean of the other semi-continuous instruments for the measurement of nitrate produced a slope of 1.19 ± 0.04, with an intercept of $-0.21 \pm 0.03\,\mu g\,m^{-3}$, and an r-value of 0.96. However, a regression of the mean semi-continuous

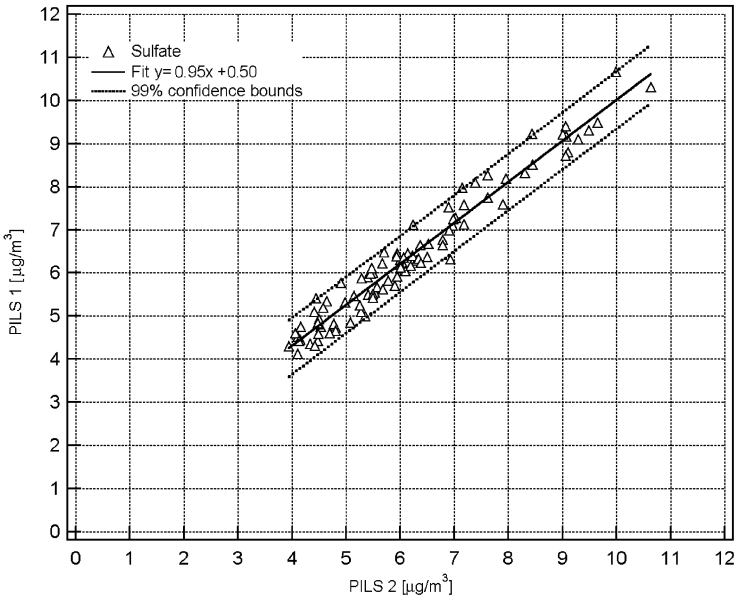

Fig. 9. Precision test made with two side-by-side 151min^{-1} PILS sampling in metro Atlanta, Georgia, August 2002.

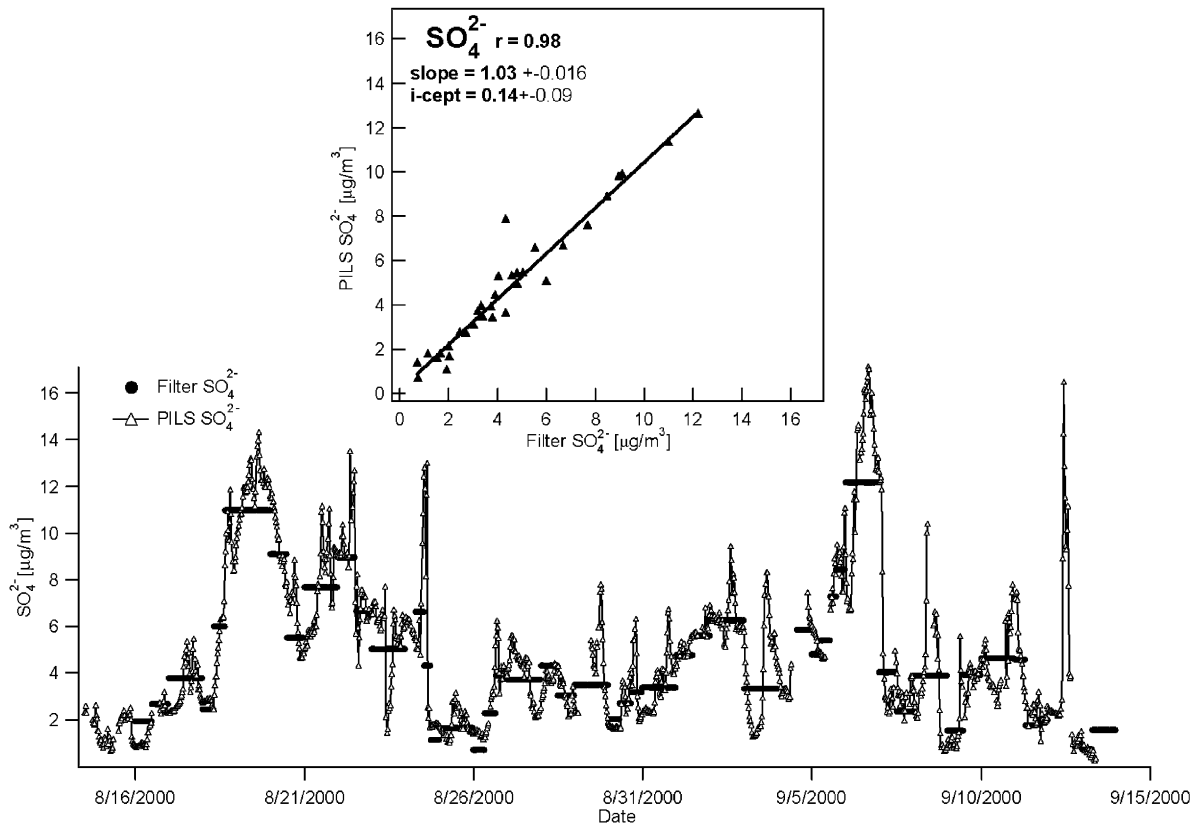

Fig. 10. $PM_{2.5}$ filter extracted sulfate versus PILS measured sulfate from Houston, Texas.

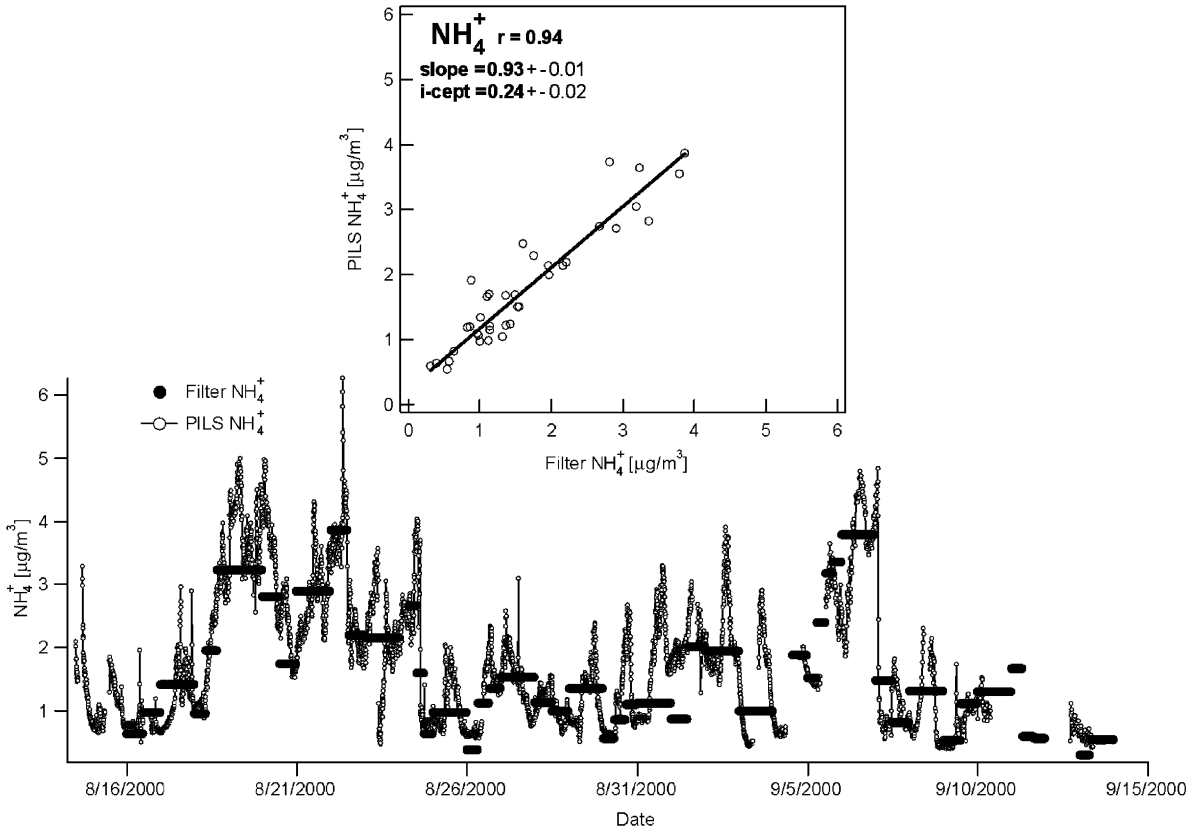

Fig. 11. $PM_{2.5}$ filter extracted ammonium versus PILS measured ammonium from Houston, Texas.

nitrate against the mean of the various filters was similarly scattered and gave an *r*-value of 0.61.

7.2. Field study results, examples from the Texas air quality study

Measurements of the soluble species in the ambient aerosol may provide insight into aerosol interactions with the gas phase, especially those influenced by changing RH. Composing an ionic charge balance from a subset of the soluble species measured rapidly and at the same time can give clues to the coupling (or not) between components. This information can suggest sources and heterogeneous conversion mechanisms that may occur on different timescales (e.g., diurnal versus passing plumes).

Fig. 13 shows a specific ion balance that includes the major inorganic soluble species as measured by the PILS in Houston, Texas. Neither sodium nor chloride were measured above the detection limit during this time period. During the daytime, relative changes in sulfate and ammonium drive the major trends in the charge balance, producing generally acidic conditions. The charge balance and nitrate concentrations show a recurring trend with aerosol nitrate corresponding with periods when the aerosol approaches neutrality (beginning of evening shaded areas between 8/19 and 8/22). Correspondingly, at the end of the shaded areas, the morning nitrate departs from the aerosol phase with the return of increased sulfate and daytime acidity. Although the charge balance shown here includes only the soluble inorganic species and is incomplete, the correspondence between nitrate and aerosol acidity is consistent with thermodynamic predictions that show nitrate concentrations in solution decrease as the solution becomes more acidic (Seinfeld and Pandis, 1998). The rapidly changing nature of the net charge during the daytime is suggestive of an aerosol whose bulk composition varies rapidly, indicating a spatially heterogeneous aerosol possibly due to mixing or influences of transport combined with an array of local sources. In contrast however, a slight nighttime diurnal rise in ammonium tracked by steady sulfate repeatedly reflects a more-neutralized aerosol.

Close inspection of the sulfate temporal trends shows that the transient sulfate events tend to display a fairly regular pattern. One representative time period is plotted in Fig. 14. The graph shows mid-day SO_2 and

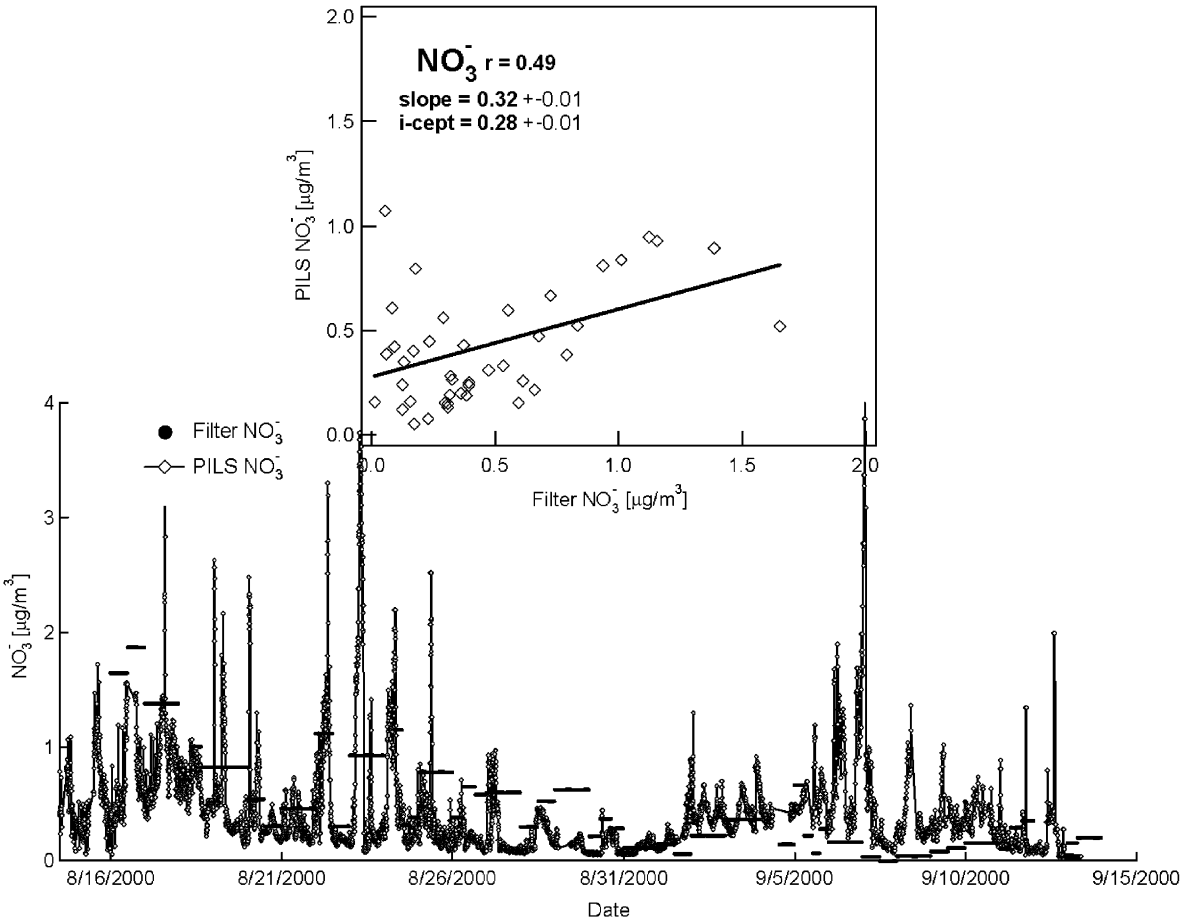

Fig. 12. $PM_{2.5}$ aerosol charge balance from inorganic ion data measured during the Texas Air Quality Study (TEXAQS 2000) in Houston.

sulfate in plumes that regularly passed over the sampling site. The shifting wind pattern, also plotted in the figure, displays a regular switch from the land to the sea breeze between the hours of 11 and 3 in the afternoon. A changing wind direction-trace indicates a changing wind speed as well, which implies varying transport times to the site. Note that during the day, the SO_2 and sulfate plumes are superimposed on what might be considered the regional sulfate.

8. PILS limitations

Some of the shortfalls in using the PILS are similar to those present in extraction of water-soluble species from filters. Although our focus is on only the soluble aerosol component, like all liquid extraction systems, the PILS approach also is susceptible to artifacts created by combining external mixtures of particles into a single liquid solution. As an example, species such as calcium sulfate have lower solubility in pure water than ammonium salts. Furthermore the insolubility increases if sulfate is added, favoring the solid phase in the following equilibrium:

$$CaSO_{4(s)} \cdot 2H_2O \langle \text{-----} \rangle Ca^{2+} + SO_4^{2-} + 2H_2O \qquad (2)$$

Thus in regions where there is an external mixture of sulfate and calcium-containing particles (e.g., dust particles), artifacts associated with solubility may confound the measurements. Although the solutions are fairly dilute in the PILS, with typical concentrations ranging from 1 to $1000\,\mu g\,l^{-1}$, the extent to which slightly soluble aerosol particles can be measured needs to be tested in the laboratory. It is possible however, to appropriately change the chemistry of the transport flow in the PILS to increase component solubility for either IC analysis or to allow for another more appropriate analytical technique. In either case, a new solvent will likely introduce new questions on specie solubility.

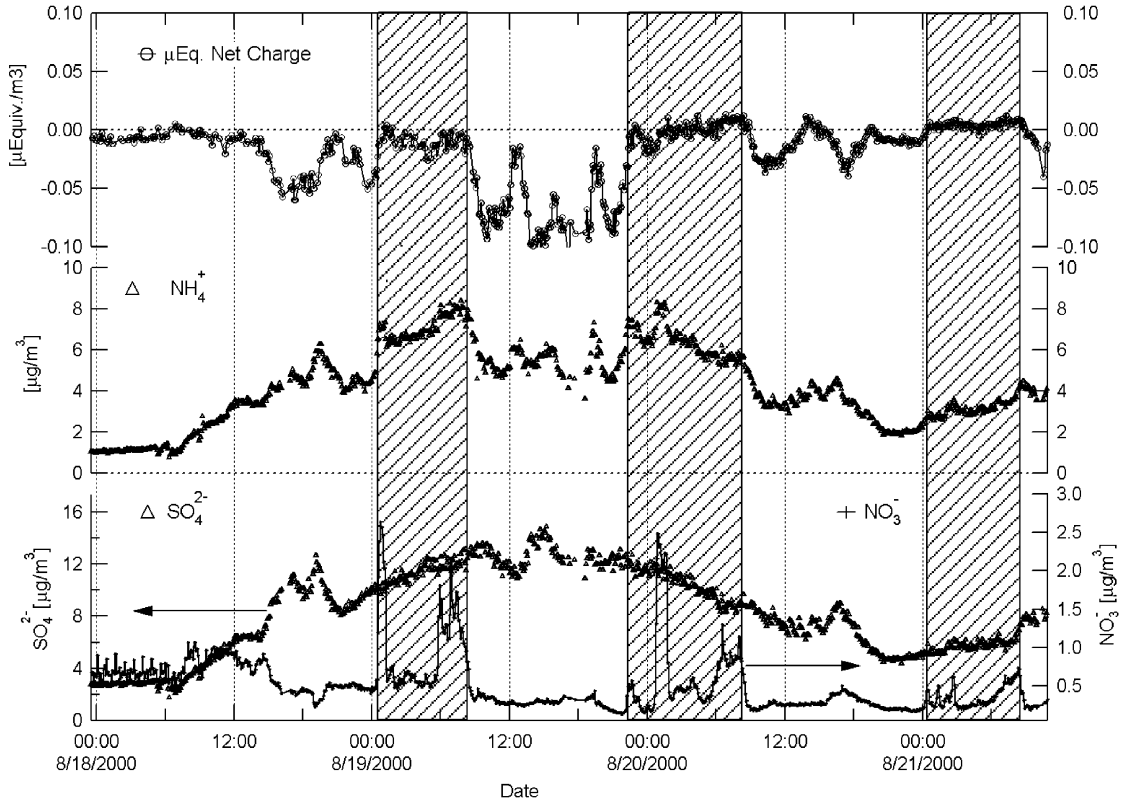

Fig. 13. $PM_{2.5}$ aerosol charge balance from inorganic ion data measured during the Texas Air Quality Study (TEXAQS, 2000) in Houston.

9. Summary

A refined $15\,l\,min^{-1}$ version of the PILS has been developed to measure the soluble species in the bulk aerosol in both ground-based and aircraft studies. Calibration aerosols generated from solutions of olive oil and fluorescein show that the PILS can collect 97% of the particle mass in a $15\,l\,min^{-1}$ sample flow, in the particle size range 30 nm–10 μm. The output of the PILS-instrument is an adjustable liquid water flow containing the soluble aerosol species to be measured. In the current PILS-IC system, a Metrohm 761 IC coupled to the PILS allows for online speciation of anion and cation species with respective LODs of 10 and $50\,ng\,m^{-3}$. With the appropriate columns and eluants, the speciation of the major aerosol inorganics is possible within 4 min, with extended times of 15–30 min allowing for soluble organic acids.

It is possible that with an alternate solvent composition and/or by adjusting the flow rate of the liquid flow produced by the PILS, coupling to other analytical methods is possible. One direction of this sort now in progress, is the coupling of the PILS to a water-based carbon analysis instrument (Sievers 8000 Turbo, Boulder CO), to measure all or some portion of the aerosol particle organic fraction at a rate of 6 min or less. In addition to analysis variations, the collection method within the PILS also has room for adaptation. Since the cavity impactor provides a continuous sample flow from a liquid droplet aerosol, the collector design of the PILS might be suited for rapid online studies of cloud droplet composition.

Acknowledgements

The authors gratefully acknowledge a number of agencies for their financial support during the development of this instrument. The US Environmental Protection Agency through the Southern Oxidant Study Cooperative Agreement CR824 849 and Grant # R 826 372 for the Southern Center for the Integrated Study of Secondary Air Pollutants, the Georgia Tech Foundation, and the State of Georgia for funding of the Fall Line Air Quality Study (FAQS). The National Science Foundation (NSF) through Grant # ATM-0080471, and the National Aeronautics and Space Administration (NASA) under Grant NCC-1-411. Thanks to Jay Turner

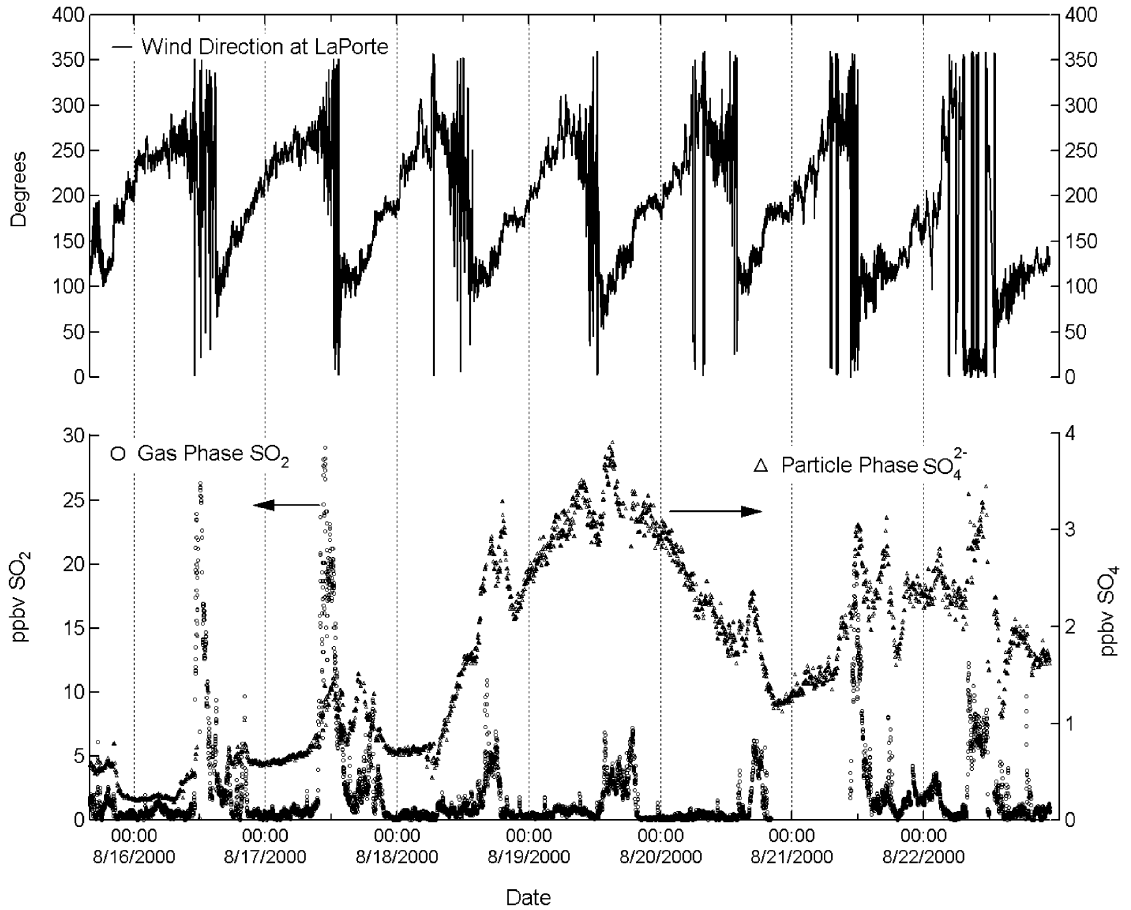

Fig. 14. $PM_{2.5}$ sulfate and SO_2 during a regular pattern of the land-sea breeze oscillation during the Texas Air Quality Study (TEXAQS, 2000) in Houston.

from Washington University, St. Louis for the VOAG-loan, and also to Rick Flagan from Cal Tech for his upside-down VOAG advice. Thanks also to Metrohm-Houston, for their cooperation in finding the appropriate columns and eluants. Finally, many thanks to Theresa Miller and Trish Quinn for help in finding the wettable quartz material for Trinidad Head.

References

Boring, C.B., Al-Horr, R., Genfa, Z., Dasgupta, P.K., 2002. Field measurement of acidic gases and soluble anions in atmospheric particulate matter using a parallel plate wet denuder and an alternating filter-based automated analysis system. Analytical Chemistry 74, 1256–1268.

Khlystov, A., Wyers, G.P., Slanina, J., 1995. The steam-jet aerosol collector. Atmospheric Environment 29, 2229–2234.

Kidwell, C.B., Ondov, J.M., 2001. Development and evaluation of a prototype system for collecting sub-hourly ambient aerosol for chemical analysis. Aerosol Science and Technology 35 (1), 596–601.

Knutson, E.O., Whitby, K.T., 1975. Aerosol classification by electrical mobility: apparatus, theory, and applications. Journal of Aerosol Science 6, 443–451.

Lim, H.-J., Turpin, B.J., Edgerton, E., Hering, S.V., Allen, G., Maring, H., Solomon, P., 2002. Semi-continuous aerosol carbon measurements: Comparison of Atlanta Supersite measurements. J. Geophys. Res. accepted for publication.

Löflund, M., Kasper-Giebl, A., Tscherwenka, W., Schmid, M., Giebl, H., Hitzenberger, R., Reischl, G., Puxbaum, H., 2001. The performance of a gas and aerosol monitoring system (GAMS) for the determination of acidic water soluble organic and inorganic gases and ammonia as well as related particles from the atmosphere. Atmospheric Environment 35, 2861–2869.

Marple, V.A., Willeke, K., 1976. Impactor design. Atmospheric Environment 10, 891–896.

Rader, D.J., Marple, V.A., 1985. Effect of ultra-stokesian drag and particle interception on impaction characteristics. Aerosol Science and Technology 4, 141–156.

Seinfeld, J., Pandis, S., 1998. Atmospheric Chemistry and Physics: From Air Pollution to Climate Change. Wiley, New York.

Sierau, B., Stratmann, F., Pelzing, M., Neususess, C., Hofmann, D., Wilke, M.A., 2002. A condensation-growth and impaction method for rapid off-line chemical-characterization of organic submicrometer atmospheric aerosol particles. Journal of Aerosol Science 34 (2), 225–242.

Simon, P.K., Dasgupta, P.K., 1995. Continuous automated measurement of the soluble fraction of atmospheric particulate matter. Analytical Chemistry 67, 71–78.

Slanina, J., Brink, H.M.t., Otjes, R.P., Even, A., Jongejan, P., Khlystov, A., Waijers-Ijpelaan, A., Hu, M., Lu, Y., 2001. The continuous analysis of nitrate and ammonium in aerosols by the steam jet aerosol collector (SJAC): extension and validation of the methodology. Atmospheric Environment 35, 2319–2330.

Stolzenburg, M.R., Hering, V., 2000. A method for the automated measurement of fine particle nitrate in the atmosphere. Environmental Science and Technology 34, 907–914.

Turpin, B.J., Cary, R.A., Huntzicker, J.J., 1990. An in situ, time-resolved analyzer for aerosol organic and elemental carbon. Aerosol Science Technology 12, 161–171.

Weber, R.J., Orsini, D., Daun, Y., Lee, Y.-N., Klotz, P., Brechtel, F., 2001. A particle-into-liquid collector for rapid measurements of aerosol chemical composition. Aerosol Science Technology 35, 718–727.

Weber, R., Orsini, D., Bergin, M., Kiang, C.S., Chang, M., John, J.S., Carrico, C.M., Lee, Y.N., Dasgupta, P., Slanina, J., Turpin, B., Edgerton, E., Hering, S., Allen, G., Solomon, P., Chameides, W., 2003a. Short-term temporal variation in PM2.5 mass and chemical composition during the Atlanta supersite experiment. Journal of Air and Waste Management Association 53, 84–91.

Weber, R.J., Orsini, D., Duan, Y., Baumann, K., Kiang, C.S., Chameides, W., Lee, Y.L., Brechtel, F., Klotz, P., Jongejan, P., Brink, H.t., Slanina, J., Dasgukpta, P., Hering, S., Stlozenburg, M., Edgerton, E., Hartsell, B., Solomon, P., Tanner, R., 2003b. Intercomparison of near real-time monitors of PM2.5 nitrate and sulfate at the EPA Atlanta supersite. Journal of Geophysical Research 1080 (D7), 10.1029/2001JD001220.

Willeke, K., Baron, P., 1997. Aerosol Measurement: Principles, Techniques, and Applications. c. Van Nostrand Reinhold.

Zellweger, C., Ammann, M., Hofer, P., Baltensperger, U., 1999. No_y speciation with a combined wet effluent diffusion denuder–aerosol collector coupled to ion chromatography. Atmospheric Environment 33 (7), 1131–1140.

Zellweger, C., Baltensperger, U., Ammann, M., Kalberer, M., Hofer, P., 1997. Continuous automated measurement of the soluble fraction of atmospheric aerosols. Journal of Aerosol Science 28 (Supplement 1), S155–S156.